Evaluation of the Residence Time Distribution (RTD) for Flow in Ducts with Velocity Profile of Two Independent Variables

Emami Meibodi, Majid*[+]

Chemical Engineering Department, Faculty of Engineering, Ardakan University, Ardakan, I.R. IRAN

ABSTRACT: *The correct information on RTD can help in system design and evaluation. The RTD corresponding to the velocity profile is known only for certain cases, where the velocity profile depends on one coordinate only. In this research, a general procedure for the derivation of RTD corresponding to a known velocity profile is introduced. The RTD of laminar flows in different ducts as elliptic, equilateral triangular, moon-shaped, and rectangular ducts are derived. Also, it is shown that the final RTD for laminar flow in any duct, can be estimated using relation $E(\theta) = K\,\theta_{min}/\theta^n$ which is similar to laminar flow in the pipe, with their own dimensionless minimum time, θ_{min}, where is defined as the required time for traveling the duct with the maximum velocity in a unit of space-time. The values of K and n are calculated to meet the condition of* $\int_{\theta_{\min}}^{\infty} E(\theta)d\theta = \int_{\theta_{\min}}^{\infty} \theta E(\theta)d\theta = \mathbf{1}$.

Besides, the values of θ_{min} for different cross-sections are studied. The results show that the RTD of elliptic ducts is precisely similar to the pipe flow. In the case of other shape ducts, the proposed model shows a suitable estimate of the numerical values. The previously published experimental data and precise analytical solutions agree with the proposed model with an acceptable consistency, except for very little time say $\theta_{min} < \theta < 0.7$.

KEYWORDS: *RTD; Velocity profile; Elliptic; Triangular; Moon-shaped; Rectangular.*

INTRODUCTION

Evaluation of RTD in various processes provides valuable information for enhancing the theoretical investigation and experimental improvement of the studied fields. The mixing efficiency was introduced using RTD to characterize the degree of mixing in a ventilation system [1]. Turbulent flows in helical static mixers were modeled by RTD [2]. Investigating the operating and design parameters of continuous powder mixers shows that the upward processing angle and low impeller rotation rate is the optimal processing setting, and these parameters result in the longest residence time and suggest that one of the main variables affecting mixing performance is residence time [3]. Some investigations attempt to link changes in filtration efficiency and pressure drop to changes in fluid RTD. The results show that a small amount of deposit yields large changes in the second moment, with the first moment remaining practically unchanged [4]. The results of the effect of compression

** To whom correspondence should be addressed.*
+ E-mail: emami@ardakan.ac.ir
1021-9986/2022/5/1715-1726 12/$/6.02

pressure in fuel cells shows that an increase in pressure leads to a translation of the RTD to smaller normalized time values. Significant attention to RTD characteristics represents a potential approach to address the development of mathematical models to design fuel cell parameters [5]. The flow dispersion level of a clean membrane of Reverse Osmosis (RO) desalination was found to be markedly affected by the presence of a fouling deposit and therefore analysis of RTD data is a novel method for online detection of membrane fouling [6]. The RTD analysis in hydro-cyclone processing copper ore leads to the determination of the kinetic parameters, degree of mixing, and relative separation of each class of grain in the hydro-cyclone [7]. It has been shown that the axial velocities in the solid separation region of the rough-cut cyclones are quite different from that conventional cyclone separators. Also, the RTD study implies a log-normal distribution for the major gas flow and a bimodal profile for the dipleg and exit tube [8]. The experimental data of an RTD study on a twin-screw extruder employed for the alkaline extraction of poplar hemicelluloses show that a reduction in screw rotation speed and solid flow rate affected the Mean Residence Time (MRT) of the liquid phase, which enhanced the extraction yield of hemicelluloses [9]. Nowadays, the radiotracer technique for the RTD measurements at industrial-scale reactors/vessels is getting popular [10–13].

Numerous studies on RTD characteristics for different applications were reported in the literature. The characterization of residence time distribution (RTD) in microreactors shows laminar flow behavior especially if the static micromixer was added to the fluidic setup [14]. Extensive studies have been reported on RTD of solute in streams and rivers and it is proved that RTD is channel size-dependent [15]. The experimental data of RTD on a high-frequency ultrasonic reactor shows that the reactor behaves like a Completely Stirred Tank Reactor (CSTR) as soon as ultrasonic operates [16]. Also, an experimental RTD study shows that the gasification technology of jet-entrained beds tends to behave like to perfect mixing process [17]. The process variables can be linked to the RTD [18]. The RTD of the liquid-phase loop reactor, taking into account the capacitance of the recycling pump [19] has a qualitatively similar trend to the closed recirculation system of a set of CSTR [20] that will approximate the RTD of a Rotating Packed Bed (RPB) system [21] for a large number of tanks. A Particulate Trajectory Model (PTM) can be used to predict RTD [22].

The relation between the velocity profile and RTD was studied *via* various viewpoints. The RTD of various forms of laminar flow of liquids in sections of vessels that are not too long was derived for flow with negligible interaction between neighboring streamlines [23]. The velocity profile derived using CFD software or velocity sensors was used to construct RTD profiles. In solid systems, the equivalent tools are the Discrete Element Method (DEM) and Positron Emission Particle Tracking (PEPT) [24]. A cell model with a place-changing probability that needs two basic inputs including a known velocity profile and a parameter for intercellular substance exchange to represent dispersion, has been used to study the influence of velocity profile and diffusion on RTD [25]. The RTD corresponding to the velocity profile of fully developed laminar flow in a straight duct with no-slip boundary conditions is known only for certain cases, where the velocity profile depends on one coordinate only. The knowledge of the RTD of laminar flow in straight channels with non-circular cross-section is not only of academic interest but of significant practical importance for microfluidic devices in general. [26]. The applicability of a so-called smart RTD (SRTD) is investigated in multiphase systems as well [27]. There are three general ways to find RTD of a system including 1- pure experimental methods such as nonreactive tracers, 2- theoretically based models beside empirical correlations such as dispersion model with axial dispersion as a function of Re and Sc, 3- pure theoretical relations such as RTDs of plug flow, completely mixed flow, and the RTD corresponding to the velocity profiles for different laminar and turbulent flows [23, 28]. It is worth noting that the corresponding RTD to the axial velocity profile is based on the pure convective assumption. In this research, the required relations for straightforward determination of RTD using velocity profiles are well formulated. The proposed algorithm is applicable to the velocity profiles of two independent variables although the final relation may not be expressed in an explicit form.

The mathematical modeling of RTD in ducts

The fraction of fluid with a flow rate between q and $(q + dq)$ and spends time between t and (t + dt) in the reactor is [29]:

$$E(t)dt = \frac{dq}{q_0} = \frac{udA_c}{u_m A_{ct}} \quad (1)$$

where u is the velocity of an element of the fluid in the axial direction (x_3) to differential cross-section $dA_c = dx_1 dx_2$, u_m is the mean velocity on the whole cross-section A_{ct} perpendicular to the axial direction. If the length of the studied vessel, L, is traveled during the time t by the element of fluid and at mean residence time, τ, by the fluid, then the velocity profile is expressed as

$$u^*(x_1, x_2) = \frac{1}{\theta} = \frac{u(x_1, x_2)}{u_m} \quad (2)$$

Where $\theta = t/\tau$ is a dimensionless time. Differentiation of logarithm of Eq. (2) result in $du^*/u^* = -d\theta/\theta$ where beside the equity of $E(t)dt = E(\theta)d\theta$ and using Eq. (1) one can derive the final equation for RTD as

$$E(\theta) = \frac{1}{\theta^3}\left|\frac{d(A_c/A_{ct})}{du^*}\right| \quad (3)$$

where the absolute operator prevents negative values for RTD. For laminar pipe flow with $u^*_{max} = 2$, the velocity profile is $u^* = 2\left[1-(r/R)^2\right]$ or $du^* = -4(r/R)d(r/R)$ and $dA_c/A_{ct} = 2(r/R)\,d(r/R)$, then Eq. (3) will be simplified to the famous $E(\theta) = 1/(2\theta^3)$ or with the definition of $\theta_{min} = 1/u^*_{max}$ it can be expressed as

$$E(\theta) = \theta_{min}/\theta^3 \quad (4)$$

In another sense of Eq. (3), A_c is the area of close loci of fluid elements with the specified value of u^*. In this view, $(r/R)^2 = 1-u^*/2$ and consequently one can write $A_c/A_{ct} = 1-u^*/2$ where Eq. (3) simply arises to Eq. (4). In the case of more complicated velocity profiles such as the velocity profiles in the ducts with the triangular or moon-shaped cross-sections that will be explained in the following section, at first the loci of constant velocity should be derived and then Eq. (3) is analytically or numerically evaluated.

In this research, it is proposed that a similar form of RTD to that of laminar pipe flow may be used to approximate other laminar flows. The proposed relationship is

$$E(\theta) = K\frac{\theta_{min}}{\theta^n} \quad (5)$$

Where the value of the exponent n and K that meet $\int_{\theta_{min}}^{\infty} E(\theta)d\theta = \int_{\theta_{min}}^{\infty} \theta E(\theta)d\theta = 1$ is derived as

$$n = \frac{2-\theta_{min}}{1-\theta_{min}} \quad (6a)$$

and

$$K = (n-1)\theta_{min}^{n-2} \quad (6b)$$

The algorithm of the calculations can be considered as follows. The velocity profiles and the corresponding relations for mean and maximum velocity are known in the literature or mathematical manipulation. The dimensionless velocity, u^*, and dimensionless maximum velocity, u^*_{max}, can be evaluated, and immediately the value of $\theta_{min} = 1/u^*_{max}$ will be specified that may be a function of some geometrical parameters of the cross-section. The corresponding n to any values of θ_{min} is calculated using Eq. (6). The proposed model, Eq. (5), is completely specified at this stage. To evaluate RTD using Eq. (3), the form of u^* as a function of A_c/A_{ct} should be known. It will be available only for a few cross-sections such as circular and elliptical ducts. For other shapes, the values of u^* at each element of cross-sections are calculated - here using a Matlab code - and the loci of the elements with the same u^* values will construct the constant velocity loci where the corresponding A_c may be evaluated numerically. The values of u* against A_c/A_{ct} will be used to evaluate RTD using Eq. (3).

RESULTS AND DISCUSSION

Here, Eq. (3) is verified for some configurations.

Laminar flow in an elliptical duct

The velocity profile of laminar flow in an elliptical duct can be expressed as [30]

$$u^* = -\frac{2}{b^2}\left(\alpha^{*2} z^2 + y^2 - b^2\right) \quad (7)$$

where $\alpha^* = b/a$, $-a \le z \le a$; $-b \le y \le b$ and the area of $A_{ct} = \pi ab$. The maximum velocity will be at the origin, $u^*_{max} = 1/\theta_{min} = 2$. The loci of the constant velocity should apply to

$$\alpha^{*2} z^2 + y^2 - b^2(1-u^*/2) = 0 \quad (8)$$

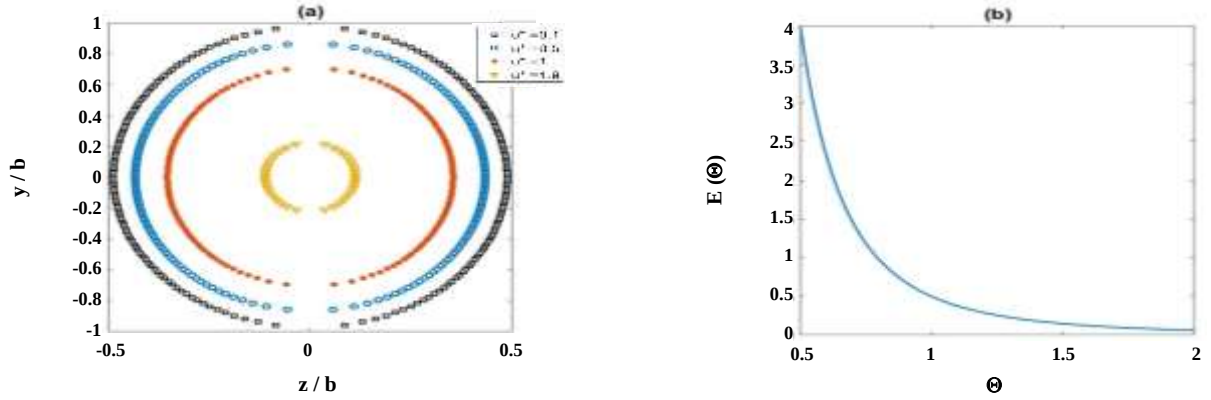

Fig. 1: The loci of the constant u* (a), and the RTD of the elliptical duct (b); that is precisely similar to the RTD of a circular pipe.

where is an elliptic similar to the duct with $a' = a\sqrt{1-u^*/2}$ and $b' = b\sqrt{1-u^*/2}$, and therefore $A_c = \pi ab(1-u^*/2)$ or $A_c / A_{ct} = 1-u^*/2$ that is the same as the circular duct. Finally, the RTD of elliptical duct flow according to Eq. (3) is precisely expressed using the laminar pipe flow, Eq. (4). Fig. 1 shows the loci of constant velocity (u^*) and the RTD of the elliptical duct. The selected value of $\alpha^* = 2$ is used for constant u^* loci in Fig. 1.

Laminar flow in an equilateral triangular duct

The velocity profile of laminar flow in an equilateral triangular duct can be expressed as [30]

$$u^* = -\frac{15}{8b^3}\left[-y^3 + 3yz^2 + 2b(y^2+z^2) - \frac{32}{27}b^3\right] \qquad (9)$$

where the height of the triangle is 2b, each side is $4b/\sqrt{3}$, the origin is set to the center of the area, $-b \le z \le b$, $-2b/3 \le y \le 4b/3$ and $A_{ct} = 4b^2/\sqrt{3}$. The maximum velocity at the origin is $u^*_{max} = 1/\theta_{min} = 20/9$. The loci of constant velocity, u* = cte, at any specified u* for each value of y will apply the following equation for z

$$\left(\frac{z}{b}\right)^2 = \frac{32/27 + (y/b)^3 - 2(y/b)^2 - (8/15)u^*}{3(y/b)+2} \qquad (10)$$

However, before taking the second root of the right-hand side of Eq. (10), negative values should be replaced by zero and after calculation of the square root, both plus and minus signs are acceptable. For plotting the calculated loci, zero values of z should be separated to have the final shape. Fig. 2 shows the loci of u* = 0.1, 1, and 2.

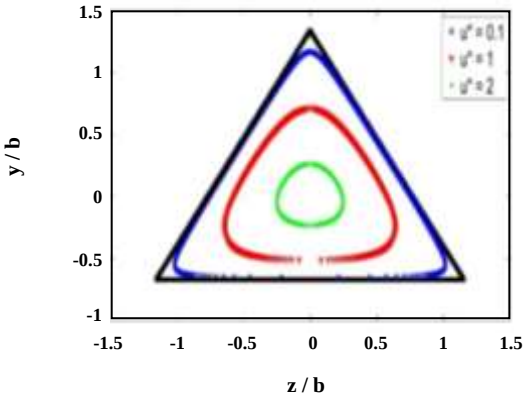

Fig. 2: The loci of constant velocity for laminar flow in an equilateral triangular duct for different values of u*.

The shape of the constant velocity loci variates as the value of u* increases and its area cannot be evaluated analytically. Nevertheless, simple numerical evaluation yield Fig. 3 for A_c/A_{ct} against u* as the required function in Eq. (3). Here a range of $10^{-3} \le u^* \le 0.99u^*_{max}$ and the whole range of y is divided into 1000 sections and each element is considered a rectangle. The calculated area is not very sensitive to the selected ranges and meshes size (e.g. 1000 is comparable to 100).

The final RTD curve according to Eq. (3) is shown in Fig. 4 which compares the derived data to Eq. (5) in which the value of n is calculated using Eq. (6) as 2.58. Although there is some deviation at high values of time, the unity Pearson correlation coefficient, $R^2 = 1$, shows a good representation of RTD by Eq. (5) without any fitted parameters.

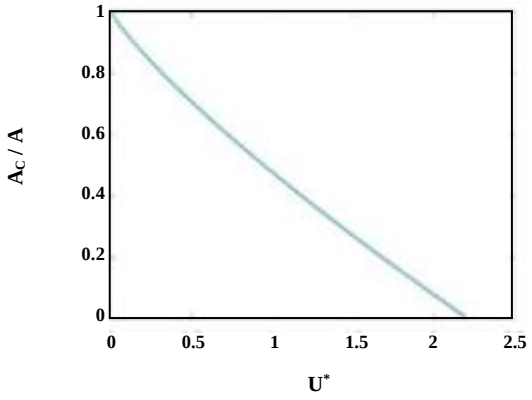

Fig. 3: The numerical evaluation of A_c/A_{ct} against u for laminar flow in an equilateral triangular duct.*

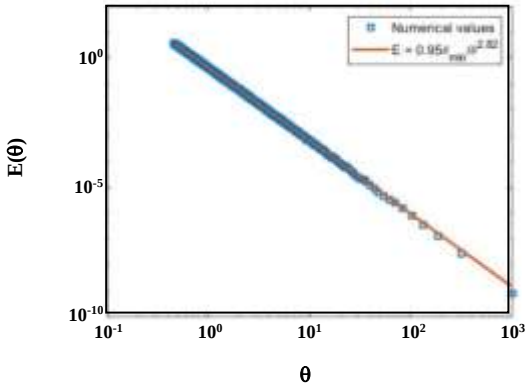

Fig. 4: The RTD of laminar flow in an equilateral triangular duct.

Laminar flow in a moon-shaped duct

The velocity profile of laminar flow in a moon-shaped duct can be expressed as [30]

$$u^* = M\left[\left(\frac{r}{a}\right)^2 - \alpha^{*2}\right]\left(1-\frac{2\cos(\hat{\theta})}{r/a}\right); \quad 0 \le \hat{\theta} \le \varphi \qquad (11)$$

where

$$M = \frac{\left(2-\alpha^{*2}\right)\varphi + \sin(2\varphi)}{\left(\alpha^{*4}/2 + 2\alpha^{*2} - 1\right)\varphi - (8/3)\alpha^{*3}\sin(\varphi) + (\alpha^{*2} - \frac{2}{3})\sin(2\varphi) - \sin(4\varphi)/12} \qquad (12)$$

and $a^* = b/a$. The nomenclatures are similar to [30] and the angle $\hat{\theta}$ should not be confused with the dimensionless time variable, θ.

The maximum velocity is calculated via

$$u^*_{max} = \frac{1}{\theta_{min}} = M\left(1+\alpha^*-\frac{3}{4}\alpha^{*2}\right)\frac{(\alpha^*/2)-1}{(\alpha^*/2)+1} \qquad (12)$$

The values of maximum velocity, θ_{min} and corresponding K and n, according to Eq. (6) against the geometric angle, φ, are depicted in Fig. 5.

The loci of the constant velocity cannot be specified analytically, however, numerical evaluation is used to derive it as shown in Fig. 6. For determination of locus for each u*, say u^*_i, at every degree of $\hat{\theta}$ the radial position for which the objective function $(1-u^*/u^*_i)^2$ is minimized, should be selected and the minimum value should be less than e.g. 10^{-4}, otherwise unwanted curve parts will connect the locus to the vertices.

According to Fig. 6, the shapes of constant velocity loci depend on the selected velocity and therefore only the numerical method is applicable for area evaluations. Nevertheless, the calculations are complicated and the selected method in this research produces some scattered data especially at lower velocities as can be seen in Fig. 7. The area of each constant velocity locus is calculated by subtracting the area of its left-hand side curve from the corresponding right-hand side.

The studied values include 500 velocity points between 0.1 to 0.99 of the maximum velocity, 500 values $\hat{\theta}$ between 0 to φ, and 500 values for r/a between α^* and $r_{out}/a = 2\cos(\hat{\theta})$. Finer meshes do not lead to more precise values. It is obvious that the calculations will produce half the area and should be doubled to have the correct value. However, a polynomial relation as

$$\frac{A_c}{A_{ct}} = -0.11u^{*2} - 0.17u^* + 1 \qquad (13)$$

can properly reproduce the area of constant velocity loci as shown in Fig. 7. It was derived by fitting the relation to the numerical data followed by rounding the coefficient as applying the condition of zero velocity, Ac(u* = 0)/Act = 1. Fig. 7 shows the data for b = 1 and $\varphi = \pi/3$, however, Eq. (13) is suitable for other values since the variation of these parameters does not have any significant effect and the nature of scattered data does not permit a precise relation. Eq. (13) facilitates using of Eq. (3) for evaluating RTD

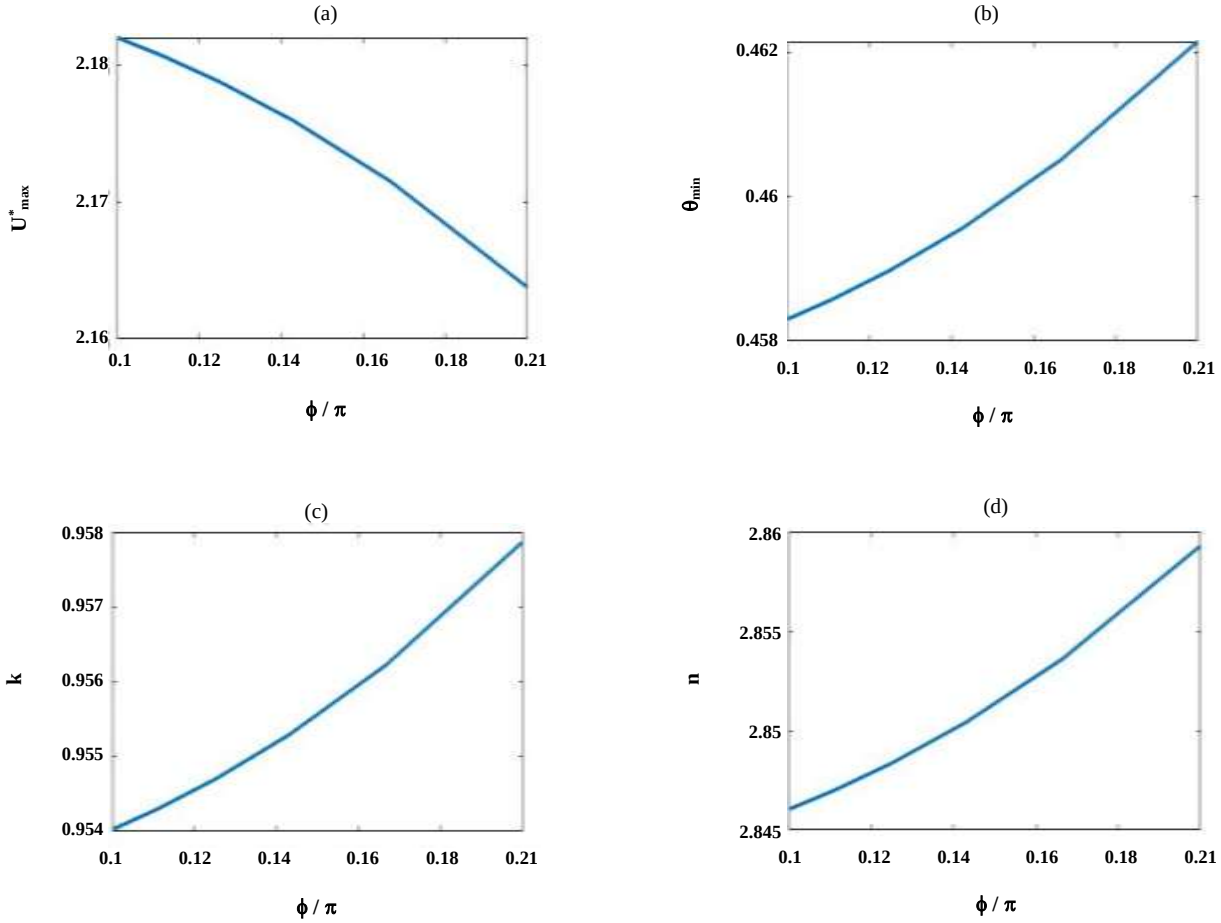

Fig. 5: The variation of a) u$_{max}$, b) θ_{min}, c) K and d) n according to Eq. (6) against φ for moon-shaped duct.*

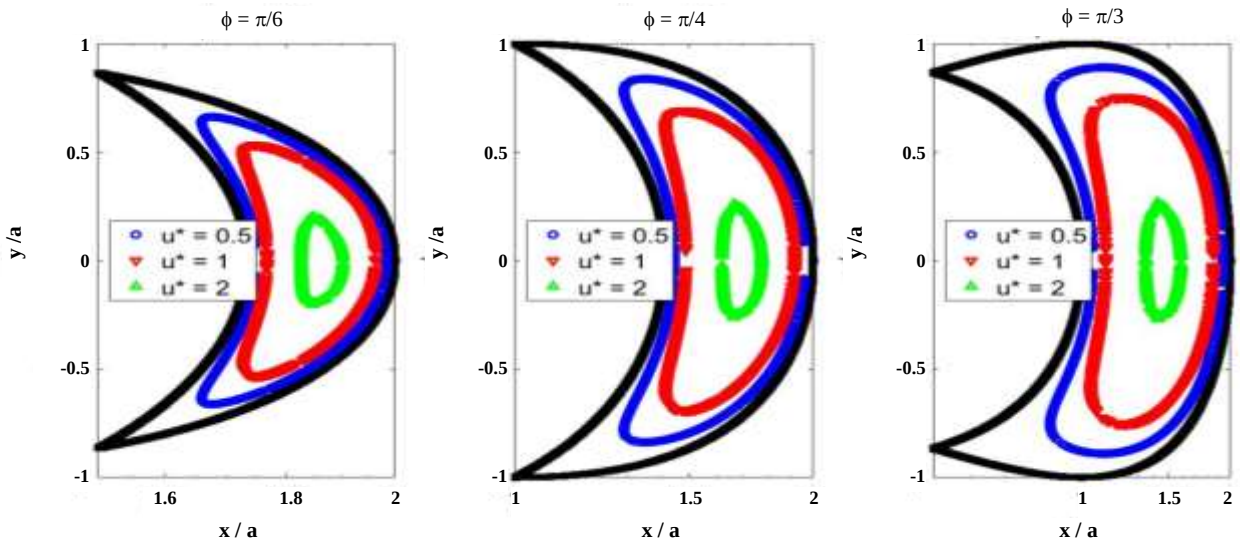

Fig. 6: The loci of constant velocity for laminar flow in a moon-shaped duct for different values of u and φ.*

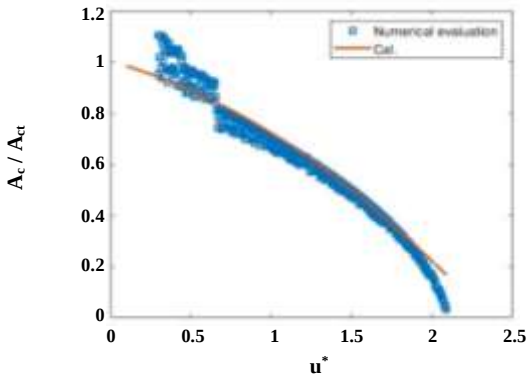

Fig. 7: The numerical evaluation of A_c/A_{ct} against u* for laminar flow in a moon-shaped duct with $\varphi = \pi/3$ and b=1.

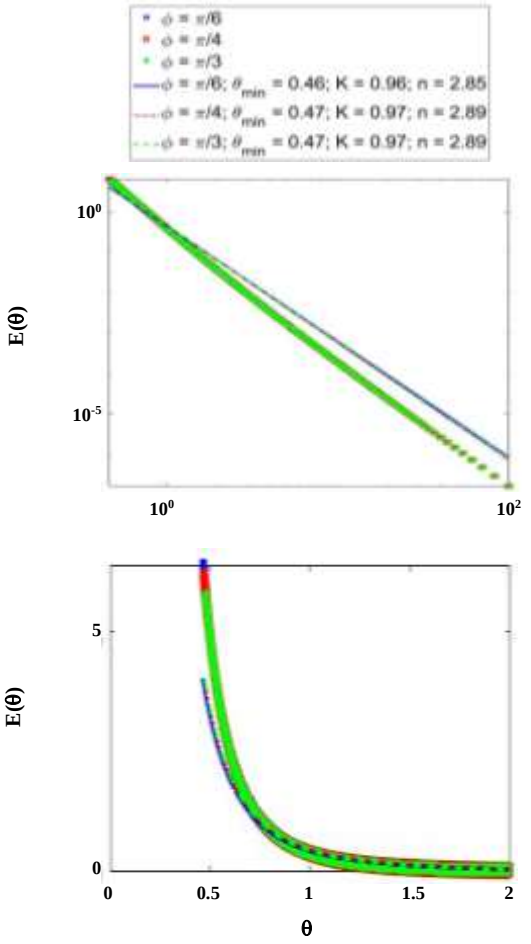

Fig. 8: The RTD of laminar flow in a moon-shaped duct.

of the flow. Fig. 8 shows the final RTD compared to the prediction of Eq. (5) with the values of θ_{min} and n that were depicted in Fig. 5. Similar to the triangular duct although some deviation is seen, the high value of the Pearson correlation coefficient, R^2 = 0.98, shows a good representation of RTD by Eq. (5) without any fitted parameters.

Laminar flow in a rectangular duct

The velocity profile of laminar flow in a rectangular duct with the horizontal length of 2a in the z-direction and vertical length of 2b in the y-direction and the origin at its center can be expressed as [30]

$$u^* = \frac{48}{\pi^3} \times \frac{\sum_{n=1,3,\ldots} \frac{1}{n^3}(-1)^{\frac{n-1}{2}} \left\{1 - \frac{\cosh\left[n\pi y/(2a)\right]}{\cosh\left[n\pi b/(2a)\right]}\right\} \cos\left[n\pi z/(2a)\right]}{1 - \frac{192}{\pi^5}\left(\frac{a}{b}\right) \sum_{n=1,3,\ldots} \frac{1}{n^5} \tanh\left[n\pi b/(2a)\right]} \quad (14)$$

The maximum velocity at the center of the rectangle is

$$u^*_{max} = \frac{48}{\pi^3} \frac{\sum_{n=1,3,\ldots} \frac{1}{n^3}(-1)^{\frac{n-1}{2}} \left\{1 - \frac{1}{\cosh\left[n\pi b/(2a)\right]}\right\}}{1 - \frac{192}{\pi^5}\left(\frac{a}{b}\right) \sum_{n=1,3,\ldots} \frac{1}{n^5} \tanh\left[n\pi b/(2a)\right]} \quad (15)$$

where depends on the ratio b/a as is shown in Fig. 9. According to this figure, the curves of the maximum velocity, minimum time, and corresponding K and n have an extremum at b/a = 1. Fig. 10 shows the contour plot for u* in the cross-section of the rectangular duct for b/a = 0.5.

Although the shape of constant velocity loci changes from a rectangle to an elliptic as the velocity increases, the numerical evaluation of the area ratio against u* results in a smooth curve as depicted in Fig. 11. Therefore, in the spite of the moon-shaped duct, a precise numerical RTD curve will be calculated as is shown in Fig. 12. Nevertheless, for studied values of b/a, the Pearson correlation coefficient for prediction of Eq. (5) does not exceed 0.89, although it is very good by eye!.

Discussion and verification of the model

According to Levenspiel [20], for the pure convection model (laminar flow in short tubes or laminar flow of viscous materials) the RTD can be derived theoretically using velocity profiles. However, verification by experiments will show the applicability of the model. The proposed model in this research is an approximate RTD for various laminar flows. Therefore, it was verified by comparing the exact RTDs.

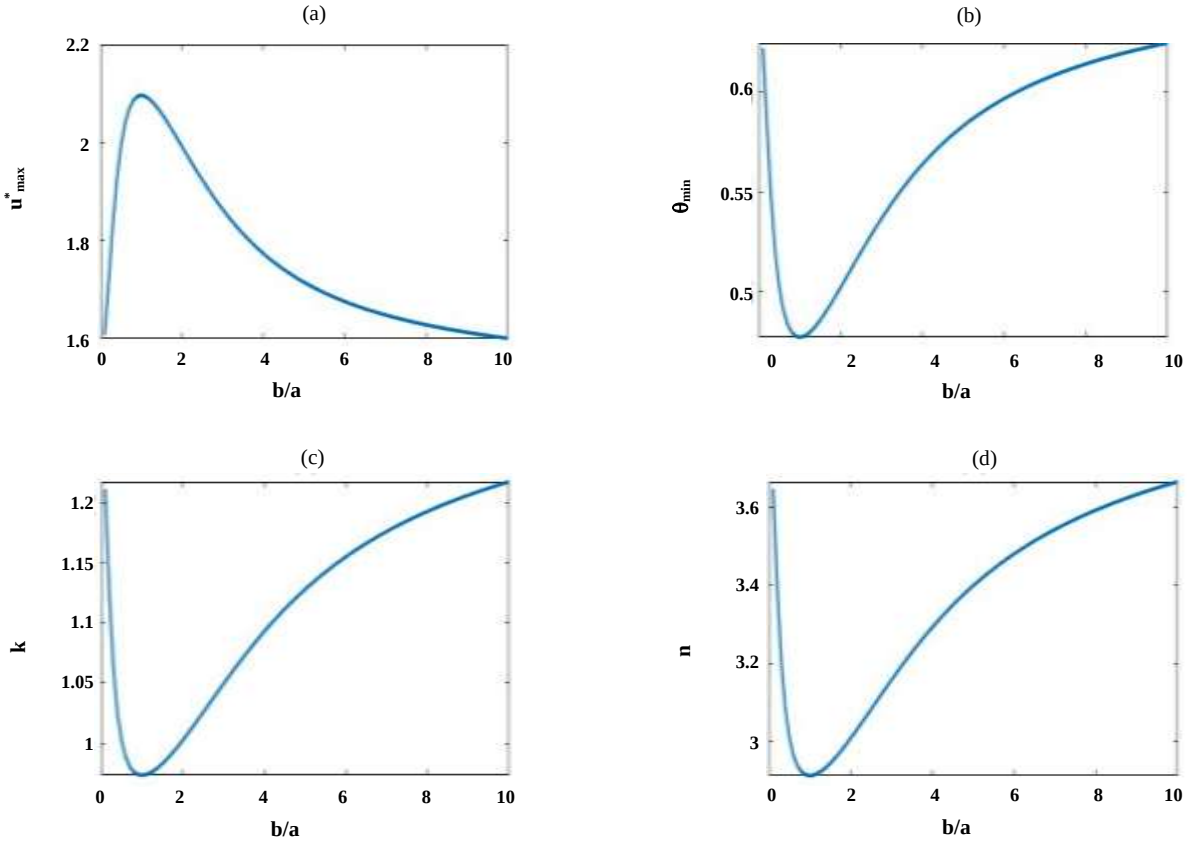

Fig. 9: The variation of a) u$_{max}$, b) θ_{min} , c) K and d) n according to Eq. (6) against b/a for rectangular duct.*

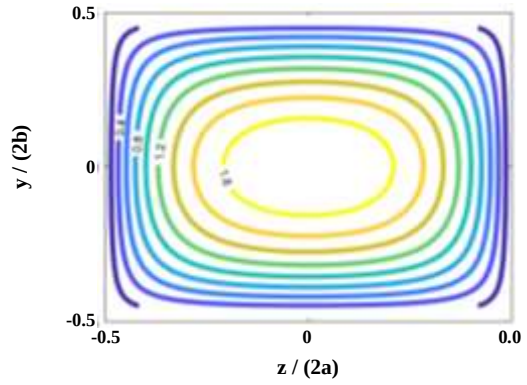

Fig. 10: The contour plot for the velocity of laminar flow in a rectangular duct with b/a = 0.5.

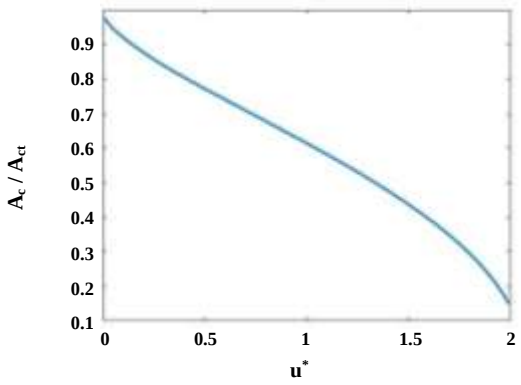

Fig. 11: The numerical evaluation of A_c/A_{ct} against u for laminar flow in a rectangular duct with b/a = 0.5.*

To test the proposed model, experimental RTD for micro-structured plate reactors was studied. *Cantu-Perez et al.* measured RTD by monitoring the concentration of a tracer dye using a LED-photodiode system [31]. Their experimental and numerical RTDs for the channel with the simple rectangular slit of width 14 mm and height 2.46 mm at a flow rate of 0.2 mL/min can be compared to the prediction of Eq. (5) in Fig. 13. The particle tracking loci in Fig. 13b were obtained based on the Navier-Stokes and the continuity equations, simultaneously with COMSOL Multiphysics 3.5 for 10,000 particles that were distributed proportionally to the axial velocity at the channel inlet.

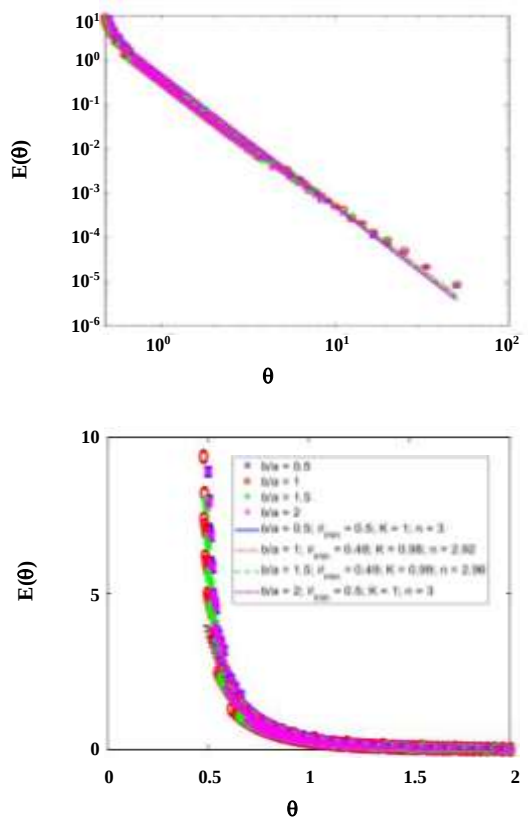

Fig. 12: The RTD of laminar flow in a rectangular duct.

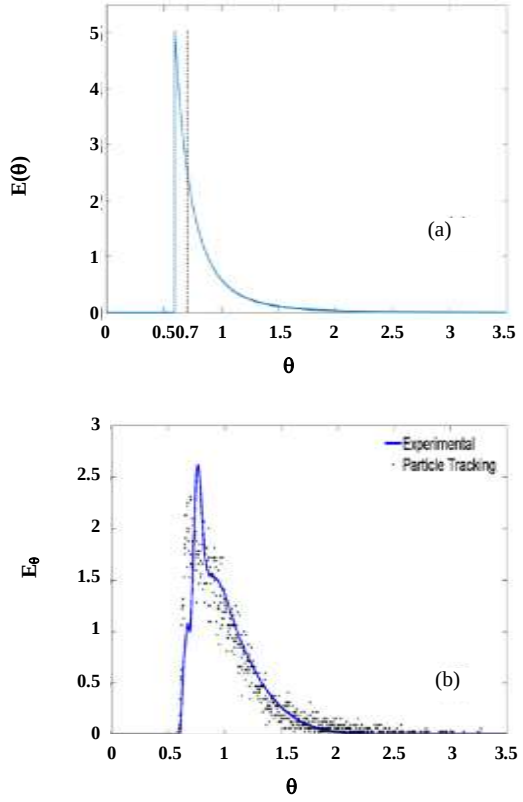

Fig. 13: prediction of (a) the proposed model compared to (b) the research of Cantu-Perez et al. [31].

No-slip boundary conditions were applied to all walls and periodic boundary conditions were considered at the inlet and outlet.

The calculations result in $\theta_{min} = 0.5921$ and $n = 3.4517$ and $K = 1.1457$ as shown in Fig. 9. As can be seen in Fig. (13b), experimental data verify the calculated value of θ_{min}. Also, the experimental RTD is consistent with the proposed model, Fig. 13a, at $\theta > 0.7$ without any adjustable parameter. However, the values of E corresponding to $0.56 < \theta < 0.7$ seems to overestimate the experimental data. Nevertheless, it may be related to the assumed velocity profile, because the approximate method used by Worner [26] verifies the proposed model and the lack of precision may be related to the difference between the actual velocity profile and Eq. (14) as the theoretical velocity profile beside the experimental error.

The proposed model is not restricted to the studied configurations. For example, Fig.14 shows the prediction of Eq. (5) compared to the precise analytical RTD for falling film flow [23] and laminar flow in annulus [32].

According to *Levenspiel et al.* [23], the value of θ_{min} for falling film flow is 2/3 and by Eq. (6) the values of model parameters are $n = 4$ and $K = 4/3$. Also, the Fig. 14 shows the laminar flow in an annulus with a selected ratio of the outside radius of the inner cylinder to the inside radius of the outer cylinder as 0.3, and the corresponding θ_{min} is evaluated according to the relations of *Pudjiono et al.* [32] as 0.6569 that according to Eq. (6) corresponds to $n = 3.9149$ and $K = 1.3037$. According to Fig. 14, the prediction of the proposed model is acceptable unless for a dimensionless time near to the θ_{min}.

The proposed model is claimed only to be approximate to the exact RTDs of various flows. The proposed RTD provides a suitable approximation to the exact ones. For example, the approximate dispersion model with derived D/uL based on the variance of experimental RTD, will not result in a dispersion model-RTD coincided with the experimental RTD. Therefore, the observed differences for $\theta > 0.7$ are acceptable.

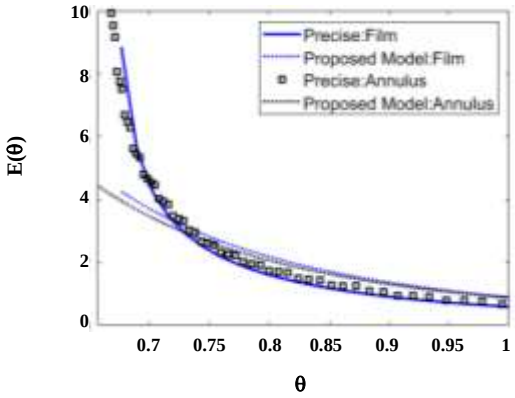

Fig. 14: The prediction of the proposed model compared to the precise analytical solution for falling film flow [23] and laminar flow in annulus [32].

CONCLUSION

The RTD of flow is usually determined experimentally. However, it can be derived analytically if the velocity profile of flow is known. The derivation method is straightforward for the axial profiles with one geometrical variable, but it is complicated in the case of profiles with two independent variables especially if its functionality is expressed by the terms containing infinite series. Some researchers used approximate methods.

In this research, a general algorithm is proposed that can be used for any velocity profile. The loci of constant velocity should be determined analytically or numerically. The laminar flow velocity profiles of four cross-section shapes were studied. In the case of laminar flow in elliptical ducts, all relations are derived analytically and the final form is precisely similar to the pipe flow. In the case of laminar flow in an equilateral triangular duct, the loci of constant velocity can be expressed analytically and its RTD was derived numerically. In the case of laminar flow in the moon-shaped duct, the loci of constant velocity were estimated by an analytical expression and its RTD was derived numerically. In the case of laminar flow in a rectangular duct, both loci of constant velocity and RTD were derived numerically.

Also, a simple relation with two parameters is proposed that the parameters are specified based on the maximum velocity and the condition of unity integral of RTD together with the definition of mean residence time. Therefore, the proposed model does not have any adjustable parameters. The previously reported experimental data of the rectangular duct and the precise analytical relations for falling film flow and annular flow verified the applicability of the proposed model.

Supporting Information

The MATLAB codes for Figs. (PDF).

Nomenclatures

a	Constant
b	Constant
A_{ct}	Total cross-section, m^2
dA_c	The area element of cross-section, m^2
D	Diffusion coefficient, m^2/s
E(t)	Residence time distribution, s^{-1}
dq	The flow rate element equal to $u.dA_c$, m^3/s
n	Constant
q_0	Total flow rate, m^3/s
R	Radius, m
r	Radial position, m
Re	Reynolds number, $Re = 2R.u_m / \nu$
Sc	Schmidt number, $Sc = \nu / D$
t	Time, s
u	Velocity, m/s
u_m	Mean velocity equal to q_0/A_{ct}, m/s
$u^* = u / u_m$	Dimensionless velocity
x_1, x_2	Geometrical dimensions of the cross area, m
y	Geometrical dimension
z	Geometrical dimensions

Greek letters

$\alpha^* = b / a$	Constant
$\theta = t / \tau$	Dimensionless time
θ_{min}	Minimum value of θ
τ	The time constant, space-time, stress
ν	Kinematic viscosity, m^2/s
φ	Angle

Received : May 14, 2021 ; Accepted : Jul. 5, 2021

REFERENCES

[1] Liao C.M., Liang H.M., A linear Model of the Effects of Residence Time Distribution on Mixing Pattern in a Ventilated Airspace, *Build. Environ.*, **38**: 11–21 (2003).

[2] Rajamanickam A., Balu K., Design and Development of Mathematical Model for Static Mixer, *Iran. J. Chem. Chem. Eng. (IJCCE)*, **35 (1)**: 109–116 (2016).

[3] Portillo P.M., Ierapetritou M.G., Muzzio F.J., Characterization of Continuous Convective Powder Mixing Processes, *Powder Technol.*, **182**: 368–378 (2008).

[4] Rodier E., Dodds J.A., Leclerc D., Clément G., Changes in Fluid Residence Time Distribution During Deep-Bed Filtration, *Chem. Eng. J.*, **68**: 131–138 (1997).

[5] St-Pierre J., Wong A., Diep J., Kiel D., Demonstration of a Residence Time Distribution Method for Proton Exchange Membrane Fuel Cell Evaluation, *J. Power Sources*, 164 (2007).

[6] Hasson D., Drak A., Komlos C., Yang Q., Semiat R., Detection of Fouling on RO Modules by Residence Time Distribution Analyses, *Desalination*, **204**: 132–144 (2007).

[7] Stegowski Z., Leclerc J.P., Determination of the Solid Separation and Residence Time Distributions in an Industrial Hydrocyclone Using Radioisotope Tracer Experiments, *Int. J. Miner. Process*, **66**: 67–77 (2002).

[8] Zhongxi C., Guogang S., Jiao J., Zheng Y., Bing G., Mingxian S., Gas Flow Behavior and Residence Time Distribution in a Rough-Cut Cyclone, *Chem. Eng. J.*, **106**: 43–52 (2005).

[9] N'Diaye S., Rigal L., Factors Influencing the Alkaline Extraction of Poplar Hemicelluloses in a Twin-Screw Reactor: Correlation with Specific Mechanical Energy and Residence Time Distribution of the Liquid Phase, *Bioresour. Technol.*, **75**: 13–18 (2000).

[10] Sheoran M., Chandra A., Bhunia H., Bajpai P.K., Pant H.J., Industrial Scale RTD Measurement Using Gold Radiotracer, *Iran. J. Chem. Chem. Eng. (IJCCE),* **40 (1)**: 313-321 (2021).

[11] Sheoran M., Goswami S., Pant H.J., Biswal J., Sharma V.K., Chandra A., Bhunia H., Bajpai P.K., Rao S.M., Dash A., Measurement of Residence Time Distribution of Liquid Phase in an Industrial-Scale Continuous Pulp Digester Using Radiotracer Technique, *Appl. Radiat. Isot.*, **111**: 10–17 (2016).

[12] Goswami S., Pant H.J., Sheoran M., Chandra A., Sharma V.K., Bhunia H., Residence Time Distribution Measurements in an Industrial-Scale Pulp Digester Using Technetium-99m as Radiotracer, *J. Radioanal. Nucl. Chem.*, **323**:1373–1379 (2020).

[13] Sheoran M., Chandra A., Bhunia H., Bajpai P.K., Pant H.J., Residence Time Distribution Studies Using Radiotracers in Chemical Industry—A Review, *Chem. Eng. Commun.*, **205**: 739-758 (2018).

[14] Günther M., Schneider S., Wagner J., Gorges R., Henkel T., Kielpinski M., Albert J., Bierbaum R., Köhler J.M., Characterisation of Residence Time and Residence Time Distribution in Chip Reactors with Modular Arrangements by Integrated Optical Detection, *Chem. Eng. J.*, **101**: 373–378 (2004).

[15] Deng Z.Q., Jung H.S., Ghimire B., Effect of Channel Size on Solute Residence Time Distributions in Rivers, *Adv. Water Resour.*, **33**: 1118–1127 (2010).

[16] Gondrexon N., Renaudin V., Petrier C., Clement M., Boldo P., Gonthier Y., Bernis A., Experimental Study of the Hydrodynamic Behaviour of a High Frequency Ultrasonic Reactor, *Ultrason. Sonochem.*, **5**: 1–6 (1998).

[17] Guangsuo Y., Zhijie Z., Qiang Q., Zunhong Y., Experimental Studying and Stochastic Modeling of Residence Time Distribution in Jet-Entrained Gasifier, *Chem. Eng. Process.*, **41**: 595-600 (2002).

[18] Galbraith S.C., Park S., Huang Z., Liu H., Meyer R.F., Metzger M., Flamm M.H., Hurley S., Yoon S., Linking Process Variables to Residence Time Distribution in a Hybrid Flowsheet Model for Continuous Direct Compression, *Chem. Eng. Res. Des.*, **153**: 85–95 (2020).

[19] Pinto J.C., Melo P.A., Biscaia J., Characterization of the Residence Time Distribution in Loop Reactors, *Chem. Eng. Sci.*, **56**: 2703–2713 (2001).

[20] Levenspiel O., "Chemical Reaction Engineering", 3rd ed., John Wiley & Sons Inc., (1998).

[21] Emami-Meibodi M., Soleimani M., Bani-Najarian S., Toward Enhancement of Rotating Packed Bed (RPB) Reactor for $CaCO_3$ Nanoparticle Synthesis, *Int. Nano Lett.*, **8**: 189-199 (2018).

[22] Li S.Q., Chi Y., Li R.D., Yan J.H., Cen K.F., Axial Transport and Residence Time of MSW in Rotary Kilns: Part II. Theoretical and Optimal Analyses, *Powder Technol.*, **126**: 228–240 (2002).

[23] Levenspiel O., Lai B.W., Chatlynne C.Y., Tracer Curves and the Residence Time Distribution, *Chem. Eng. Sci.*, **25**: 1611–1613 (1970).

[24] Gao Y., Muzzio F.J., Ierapetritou M.G., A Review of the Residence Time Distribution (RTD) Applications in Solid Unit Operations, *Powder Technol.*, **228**: 416–423 (2012).

[25] Steffani K., Platzer B., Influence of Velocity Profile and Diffusion on Residence Time Distributions: Mesoscopic Modeling and Application to Poiseuille Flow, *Chem. Eng. Process.*, **41**:143–155 (2002).

[26] Wörner M., Approximate Residence Time Distribution of Fully Develop Laminar Flow in a Straight Rectangular Channel, *Chem. Eng. Sci.*, **65**: 3499–3507 (2010).

[27] Simcik M., Ruzicka M.C., Mota A., Teixeira J.A., Smart RTD for Multiphase Flow Systems, *Chem. Eng. Res. Des.*, **90**: 1739–1749 (2012).

[28] Emami Meibodi M., Application of Axial Velocity Profile in Order to Develop Residence Time Distribution (RTD) for Different Laminar and Turbulent Flows, *Iran. J. Chem. Chem. Eng. (IJCCE),* **41 (2)**: 493-500 (2021).

[29] Scott Fogler H., "Elements of Chemical Reaction Engineering", Prentice Hall (2006)

[30] Shah R.K., London A.L., "Laminar Flow Forced Convection in Ducts: A Source Book for Compact Heat Exchanger Analytical Data", Academic Press, New York, NY (1978).

[31] Cantu-Perez A., Bi S., Barrass S., Wood M., Gavriilidis A., Residence Time Distribution Studies In Microstructured Plate Reactors, *Appl. Therm. Eng.*, *Pergamon*, 634–639 (2011).

[32] Pudjiono P.I., Tavare N.S., Garside J., Nigam K.D. P., Residence Time Distribution from a Continuous Couette Flow Device, *Chem. Eng. J.*, **48**: 101-110 (1992).